



Thermal Functions of Diatomic Molecules Using Hulthén Plus Screened Kratzer Potential

Ahmad Ghanbari¹ · Seyedeh Media Jadbaba¹

Received: 6 October 2022 / Accepted: 20 February 2023 / Published online: 17 March 2023

© The Author(s), under exclusive licence to Springer Science+Business Media, LLC, part of Springer Nature 2023

Abstract

In the present paper, we have studied analytically the thermodynamic properties of diatomic molecules like LiH, HCl and H₂ and compared calculated properties with experimental data. In this regard, we have solved the Schrödinger equation with Hulthén plus screened Kratzer potential using the Nikiforov–Uvarov method and obtained energy eigenvalues. According to calculated the energy eigenvalues, we have deduced the partition function and thermodynamic properties of the molecules by applying the Poisson summation formalism. Our results show that the specific heat at constant pressure, Gibbs free energy and enthalpy are in good agreement with experimental data. The average deviation of the specific heat at constant pressure, Gibbs free energy and enthalpy is 1.62%, 3.57% and 4.21%, respectively. It is obvious from the data that the potential model predicts well the thermodynamic properties of diatomic molecules.

Keywords Thermodynamic function · Diatomic molecules · Hulthén plus screened Kratzer potential · Nikiforov–Uvarov method

1 Introduction

The theoretical prediction of the thermal properties of diatomic molecules is an interesting subject in physics, chemistry, material science and engineering. Examples of thermal properties are entropy, enthalpy, free energy, and specific heat [1–6]. The properties have important roles in phase transition, adsorption and synthesis of materials [7–10].

In the past few years, obtaining the thermodynamic properties of systems like diatomic molecules and semiconductors has been widely interested among scientists [2, 11–15]. The most important parameter that has played a great role in calculating

✉ Ahmad Ghanbari
ah2_ghanbari@yahoo.com

¹ University of Applied Science and Technology, Center of Gachsaran2, Gachsaran, Iran

the properties is the partition function which one can deduce it using energy eigenvalues. Applying calculated energy eigenvalues, we can obtain other thermodynamic properties such as entropy, mean energy, specific heat, and enthalpy. To this end, the first step to derive the energy spectrum is solving the Schrödinger equation [16–18] or using the path integral formalism [19, 20]. In this regard, different potential models have been studied in the literature [1, 21–27]. Among the considered potential, the Morse potential was the first experimental model that was greatly applied in physics and chemistry [28–30]. The potential is an interatomic model that generally uses the potential energy of a diatomic molecule. Therefore, many works considered other improved and generalized potentials and correspondingly derive thermodynamic properties for different systems like diatomic molecules [31–33] and nanostructures, i.e., quantum dots and quantum wires [34–36]. It is worthy to mention that the potential functions have been of growing interest because of their high application in fields like derive thermodynamic properties, calculating the molecular energy spectrum and simulation behavior of the molecular potential.

Nath and Roy [37] solved the Schrödinger equation with Deng-Fan potential using the Nikiforov–Uvarov method and obtained energy eigenvalues and thermodynamic properties for diatomic molecules such as H_2 , LiH, HCl and CO. Okorie et al. [38] calculated analytically the fractional Schrödinger equation under Morse potential and derived the partition function and thermodynamic properties like internal energy, free energy, entropy and specific heat for diatomic molecules. Ding et al. [39] predicted thermodynamic properties for the sulfur dimer. They represented a new method with temperature and pressure as independent parameters for the Gibbs free energy and entropy of the sulfur dimer. Okon et al. [40] obtained the energy spectrum and thermodynamic properties of two molecules, namely CO and SeF, in the presence of Mobius square plus screened Kratzer potential. In this regard, we have considered the Hulthén and screened Kratzer potential model and deduce energy eigenvalues and have correspondingly obtained the partition function and thermodynamic properties of the diatomic molecules such as HCl, LiH and H_2 .

As mentioned above, we combine Hulthén plus screened Kratzer (HSK) potential and have solved the Schrödinger equation applying Nikiforov–Uvarov (expressed in appendix) and series expansion method for the potential. The importance of combining potential models is obtaining a better result because potential models with more fitting quantities tend to give a better result [41, 42]. The HSK potential is defined as

$$V(r) = -\frac{Z_1 e^{vr}}{1 - e^{-vr}} - \frac{Z_2 e^{-vr}}{r} + \frac{Z_3 e^{-vr}}{r^2} \quad (1)$$

where Z_1 is the potential strength for Hulthén, and ν is the screening parameter. $Z_2 \equiv 2D_e r_e$ and $Z_3 \equiv D_e r_e^3$ where D_e and r_e are dissociation energy and equilibrium bond length, respectively. The behavior of the potential is plotted in Fig. 1.

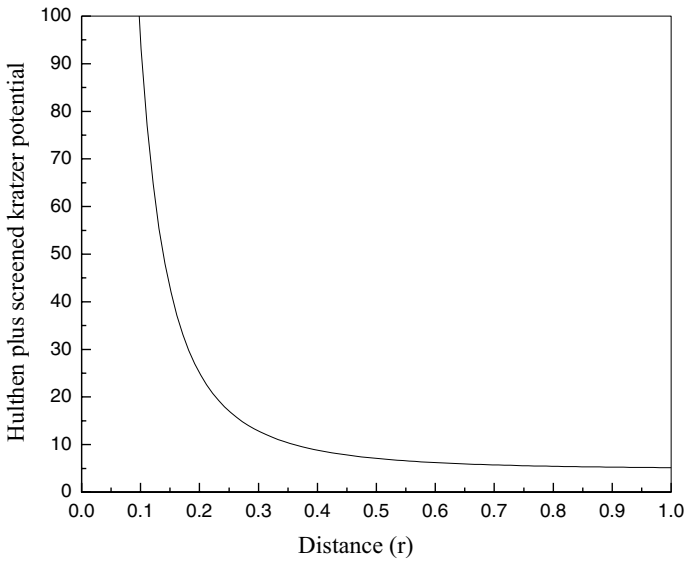


Fig. 1 Hulthen plus screened Kratzer potential as a function of distance

2 Mathematical Framework

The Schrödinger equation with HSK potential is given as

$$\left(-\frac{\hbar^2}{2\mu} \nabla^2 + V(r) \right) \Psi_{nl}(r) = E_{nl} \Psi_{nl}(r) \tag{2}$$

Where $\Psi_{nl}(r)$ denotes the eigen functions, E_{nl} shows the energy eigenvalues, μ is the reduced mass, \hbar is the reduced Plancks constant, and r is radial distance from the origin. Inserting Eq. (1) into Eq. (2), we have the following equation

$$\frac{d^2\Psi_{nl}(r)}{dr^2} + \left[\frac{2\mu E_{nl}}{\hbar^2} + \frac{2\mu Z_1 e^{-vr}}{\hbar^2(1 - e^{-vr})} + \frac{2\mu Z_2 e^{-vr}}{\hbar^2 r} - \frac{2\mu Z_3 e^{-vr}}{\hbar^2 r^2} - \frac{l(l+1)}{r^2} \right] \Psi_{nl}(r) = 0 \tag{3}$$

To release the centrifugal term in Eq. (3), we use the Greene–Aldrich approximation scheme [43]. This scheme is a proper approximation to the centrifugal term which is valid for $v \ll 1$ and it is presented as

$$\frac{1}{r^2} \approx \frac{v^2}{(1 - e^{-vr})^2} \tag{4}$$

Substituting Eq. (4) into Eq. (3), we have

$$\frac{d^2\Psi_{nl}(r)}{dr^2} + \left[\frac{2\mu E_{nl}}{\hbar^2} + \frac{2\mu Z_1 e^{-vr}}{\hbar^2(1 - e^{-vr})} + \frac{2\mu Z_2 v e^{-vr}}{\hbar^2(1 - e^{-vr})} - \frac{2\mu Z_3 v^2 e^{-vr}}{\hbar^2(1 - e^{-vr})^2} - \frac{v^2 l(l+1)}{(1 - e^{-vr})^2} \right] \Psi_{nl}(r) = 0 \tag{5}$$

For simplicity, we use the following substitution

$$y = e^{-vr} \quad (6)$$

Differentiating Eq. (6) and putting in Eq. (5), we have the following equation

$$\frac{d^2\Psi(y)}{dy^2} + \frac{1-y}{y(1-y)} \frac{d\Psi(y)}{dy} + \frac{1}{y^2(1-y)^2} [-(\varepsilon + \eta_0)y^2 + (2\varepsilon + \eta_0 - \eta_1)y - (\varepsilon + \gamma)]\Psi(y) = 0 \quad (7)$$

where

$$-\varepsilon = \frac{2\mu E_{nl}}{v^2\hbar^2}; \eta_0 = \frac{2\mu Z_1}{v^2\hbar^2} + \frac{2\mu Z_2}{v\hbar^2}; \eta_1 = \frac{2\mu Z_3}{\hbar^2}; \gamma = l(l+1); \quad (8)$$

According to Eqs. (7) and (9) of ref. [44], we have

$$\begin{aligned} \tilde{\tau} &= 1-y; \sigma(y) = y(1-y); \sigma'(y) = 1-2y; \sigma''(y) = -2; \\ \tilde{\sigma}(y) &= -(\varepsilon + \eta_0)y^2 + (2\varepsilon + \eta_0 - \eta_1)y - (\varepsilon + \gamma); \end{aligned} \quad (9)$$

Inserting Eq. (9) into Eq. (11) of ref. [44], the following equation is obtained

$$\pi(y) = -\frac{y}{2} \pm \sqrt{(B_1 - K)y^2 + (K + B_2)y + B_3} \quad (10)$$

where

$$B_1 = \left(\frac{1}{4} + \varepsilon_0 + \eta_0\right); B_2 = -(2\varepsilon - \eta_0 - \eta_1); B_3 = (\varepsilon + \gamma); \quad (11)$$

In Eq. (11), we take the discrimination under the square root sign and solve for K . Here, we consider the negative root for the bound state as

$$K = -(B_2 + 2B_3) - 2\sqrt{B_3}\sqrt{B_3 + B_2 + B_1} \quad (12)$$

By inserting Eq. (12) into Eq. (10), we have the following relation

$$\pi(y) = -\frac{y}{2} - \left[\left(\sqrt{B_3} + \sqrt{B_3 + B_2 + B_1} \right) y - \sqrt{B_3} \right] \quad (13)$$

Applying Eqs. (9) and (12), we deduce $\tau(y)$ and $\tau'(y)$ as below

$$\tau(y) = 1 - 2y - 2y\sqrt{B_3} - 2y\sqrt{B_3 + B_2 + B_1} + 2\sqrt{B_3} \quad (14)$$

$$\tau'(y) = -2 \left[1 + \sqrt{B_3} + \sqrt{B_3 + B_2 + B_1} \right] \quad (15)$$

We define λ_n and λ by referring to Eqs. (10) and (13) of ref. [44] as

$$\lambda_n = n^2 + n \left[1 + 2\sqrt{B_3} + 2\sqrt{B_3 + B_2 + B_1} \right] \quad n = 0, 1, 2, \dots \quad (16)$$

$$\lambda = -\frac{1}{2} - \sqrt{B_3} - \sqrt{B_3 + B_2 + B_1} - (B_2 + 2B_3) - 2\sqrt{B_3}\sqrt{B_3 + B_2 + B_1} \quad (17)$$

Linking Eqs. (16) and (17) with the help of Eq. (8), we can calculate the energy eigenvalues for the HSK as

$$E_{nl} = \frac{v^2 \hbar^2 l(l+1)}{2\mu} - \frac{v^2 \hbar^2}{8\mu} \left[\frac{(n + \frac{1}{2} + \sqrt{(l + \frac{1}{2})^2 + \frac{2\mu D_e r_e^2}{\hbar^2}})^2 - \frac{2\mu Z_1}{v^2 \hbar^2} + \frac{4\mu D_e r_e}{v \hbar^2} + l(l+1)}{n + \frac{1}{2} + \sqrt{(l + \frac{1}{2})^2 + \frac{2\mu D_e r_e^2}{\hbar^2}}} \right]^2 \quad (18)$$

According to the obtained energy spectrum, we calculated the partition function and thermodynamic properties of diatomic molecules. The partition function is derived by summation over all possible states of the system as

$$Q = \sum_{n=0}^N e^{-\beta E_n} \quad (19)$$

where $\beta = \frac{1}{k_B T}$, k_B shows the Boltzmann constant, and T is the temperature. Here, we have considered the s-wave state so $l = 0$ and the maximum value of N in Eq. (19) can be obtained by setting $\frac{dE_n}{dn} = 0$. Therefore, we have

$$N = \frac{-\frac{1}{2}v\hbar - \frac{1}{2}v\hbar\sqrt{\frac{\hbar^2 + 8\mu D_e r_e^2}{\hbar^2}} + \sqrt{2\mu Z_1 - 4\mu D_e r_e v}}{v\hbar} \quad (20)$$

The partition function of the system with the help of Eqs. (19) and (20) has been calculated as

$$Q = \frac{e^{8\beta v^2 \hbar^2 \left[\left(\frac{3}{2} + \frac{1}{2} \sqrt{1 + \frac{8\mu D_e r_e^2}{\hbar^2}} \right)^2 - \frac{2\mu Z_1}{v^2 \hbar^2} + \frac{4\mu D_e r_e}{v \hbar^2} \right] \left(3 + \sqrt{1 + \frac{8\mu D_e r_e^2}{\hbar^2}} \right)}}{e^{\left(\frac{3 + \sqrt{\frac{\hbar^2 + 8\mu D_e r_e^2}{\hbar^2}} \right)^2}} \left(\frac{v^2 \hbar^2 \left[\left(\frac{3}{2} \beta + \frac{1}{2} \sqrt{1 + \frac{8\mu D_e r_e^2}{\hbar^2}} \right)^2 - \frac{2\mu Z_1}{v^2 \hbar^2} + \frac{4\mu D_e r_e}{v \hbar^2} \right]^2}{\mu \beta \left(3 + \sqrt{\frac{\hbar^2 + 8\mu D_e r_e^2}{\hbar^2}} \right)^2} + \frac{16v^2 \hbar^2 \beta \left[\left(\frac{3}{2} + \frac{1}{2} \sqrt{1 + \frac{8\mu D_e r_e^2}{\hbar^2}} \right)^2 - \frac{2\mu Z_1}{v^2 \hbar^2} + \frac{4\mu D_e r_e}{v \hbar^2} \right]^2}{\left(3 + \sqrt{\frac{\hbar^2 + 8\mu D_e r_e^2}{\hbar^2}} \right)^3} \right)} \quad (21)$$

Also, the thermodynamic properties of diatomic molecules can be calculated applying the following formulas:

- Mean energy $U = -\frac{\partial \ln(Q)}{\partial \beta}$
- Entropy $S = k_B \ln(Q) - k_B \beta \frac{\partial \ln(Q)}{\partial \beta}$
- Enthalpy $H = U + PV$
- Specific heat in constant pressure $c_P = \frac{\partial H}{\partial T}$
- Specific heat in constant volume $c_V = \frac{\partial U}{\partial T}$

Table 1 Spectroscopic values of HCl, LiH and H₂

| Molecules | $D_e(eV)$ | $\nu(\text{\AA}^{-1})$ | $r_e(\text{\AA})$ | $\mu(meV)$ |
|----------------|-----------|------------------------|-------------------|------------|
| HCl | 4.6190 | 1.86770 | 1.2746 | 0.0912 |
| LiH | 2.5152 | 1.12800 | 1.5946 | 0.0819 |
| H ₂ | 4.7446 | 1.94260 | 0.7416 | 0.0502 |

Table 2 Bound state energy spectra E_{nl} of HSKP for HCl, LiH and H₂

| n | l | $E_{nl}(eV)$ | | |
|-----|-----|--------------|--------------|----------------|
| | | HCl | LiH | H ₂ |
| 0 | 0 | -22.17032494 | -9.044861721 | -13.92974441 |
| 0 | 1 | -22.17022128 | -9.044847651 | -13.93464244 |
| 0 | 2 | -22.17001432 | -9.044819582 | -13.94456401 |
| 0 | 3 | -22.16970474 | -9.044777634 | -13.94456401 |
| 0 | 4 | -22.16929354 | -9.044722014 | -13.98060726 |
| 0 | 5 | -22.16878209 | -9.044652964 | -13.98060745 |
| 1 | 0 | -22.24690799 | -9.033844252 | -13.79739618 |
| 1 | 1 | -22.24679078 | -9.033836790 | -13.80084636 |
| 1 | 2 | -22.24655670 | -9.033821914 | -13.80786295 |
| 1 | 3 | -22.24620649 | -9.033799708 | -13.81867833 |
| 1 | 4 | -22.24574126 | -9.033770284 | -13.83364106 |
| 1 | 5 | -22.24516244 | -9.033733821 | -13.85321597 |
| 2 | 0 | -22.33432382 | -9.029306244 | -13.70661022 |
| 2 | 1 | -22.33419477 | -9.029304880 | -13.70872277 |
| 2 | 2 | -22.33393705 | -9.029302176 | -13.71305549 |
| 2 | 3 | -22.33355145 | -9.029298171 | -13.71982357 |
| 2 | 4 | -22.33303911 | -9.029292928 | -13.72934979 |
| 2 | 5 | -22.33240157 | -9.029286529 | -13.74206457 |

- Free energy $F = -k_B T \ln(Q)$

3 Results and Discussion

In this section, we have studied the energy spectrum and thermodynamic properties of diatomic molecules such as HCl, LiH and H₂ under the HSK potential model. The considered potential is plotted in Fig. 1. Also, we have compared our theoretical calculated data with experimental data in NIST [45]. To this end, the spectroscopic values of the molecules are presented in Table 1 and taken from ref. [46]. In our mathematical computations, we have used the following values: $\hbar c = 1973eV\text{\AA}$ and $1amu = 931.494028eV(\text{\AA})^{-1}$ [46].

Table 3 Thermodynamic properties for HCl using Hulthen-screened Kratzer potential compared with experimental data [45]

| Temperature (K) | C_p (J/mol*K) | | $-(G-H_{298.15})/T$ (J/mol*k) | | $H-H_{298.15}$ (kJ/mol) | |
|-----------------|-----------------|-------------|-------------------------------|-------------|-------------------------|-------------|
| | Exp | Our results | Exp | Our results | Exp | Our results |
| 300 | 29.14 | 29.67 | 186.9 | 187.5 | 0.05 | 0.06 |
| 400 | 29.17 | 29.71 | 188.0 | 188.6 | 2.97 | 3.01 |
| 500 | 29.31 | 29.89 | 190.2 | 190.7 | 5.89 | 5.99 |
| 600 | 29.58 | 30.12 | 192.6 | 193.1 | 8.83 | 8.98 |
| 700 | 29.99 | 30.36 | 195.1 | 195.7 | 11.81 | 12.02 |
| 800 | 30.49 | 30.85 | 197.4 | 197.9 | 14.84 | 14.99 |
| 900 | 31.05 | 31.47 | 199.7 | 200.4 | 17.91 | 18.06 |
| 1000 | 31.63 | 31.99 | 201.9 | 202.5 | 21.05 | 21.21 |
| 1500 | 34.10 | 34.51 | 211.2 | 211.8 | 37.51 | 37.87 |
| 2000 | 35.59 | 35.97 | 218.8 | 219.6 | 54.96 | 55.34 |
| 2500 | 36.55 | 37.03 | 225.1 | 226 | 73.01 | 73.55 |
| 3000 | 37.24 | 37.96 | 230.5 | 231.7 | 91.47 | 91.89 |
| 3500 | 37.76 | 38.33 | 235.3 | 236.7 | 110.2 | 110.78 |
| 4000 | 38.15 | 38.82 | 239.6 | 240.8 | 129.2 | 130.04 |
| 4500 | 38.47 | 39.22 | 243.4 | 244.2 | 148.4 | 148.96 |
| 5000 | 38.75 | 39.56 | 246.9 | 247.8 | 167.7 | 168.32 |
| 5500 | 39.02 | 39.87 | 250.1 | 251.1 | 187.1 | 187.87 |
| 6000 | 39.31 | 40.03 | 253.1 | 253.2 | 206.7 | 207.25 |

Table 2 represents the numerical calculation of the energy spectra of the HSK for HCl, LiH and H₂. We can observe from the data that for each vibrational quantum number, the energy increases with enhancement in the rotational quantum number.

The specific heat at constant pressure, Gibbs free energy and enthalpy for HCl, LiH and H₂ are given in Tables 3, 4, and 5, respectively. The calculated data are obtained in the temperature range for HCl and H₂ at 300 K–6000 K and for LiH at 2000K–6000K. For accuracy of our computations, we have compared the results with empirical data from the NIST database. It is worth noting that according to the NIST database, the empirical values of enthalpy are represented in the reduced form $H - H_{298.15}$. Moreover, we deduce the average absolute deviation (σ_{ave}) to quantitatively analyze the accuracy of the considered potential model. For this purpose, we apply the following formula

$$\sigma_{ave} = \frac{100}{N_p} \sum \left| 1 - \frac{X_{theoretical}}{X_{experimental}} \right|$$

where N_p shows the number of data points. The average deviation of the specific heat at constant pressure, Gibbs free energy and enthalpy is 1.62%, 3.57% and 4.21%, respectively. It is obvious from the data that the potential model predicts well the thermodynamic properties of diatomic molecules.

Table 4 Thermodynamic properties for LiH using Hulthen-screened Kratzer potential compared with experimental data [45]

| Temperature (K) | C_p (J/mol*K) | | $-(G-H_{298.15})/T$ (J/mol*k) | | $H-H_{298.15}$ (kJ/mol) | |
|-----------------|-----------------|-------------|-------------------------------|-------------|-------------------------|-------------|
| | Exp | Our results | Exp | Our results | Exp | Our results |
| 2000 | 38.51 | 38.62 | 205.9 | 206.81 | 60.87 | 61.76 |
| 2100 | 38.66 | 38.74 | 207.4 | 208.12 | 64.73 | 65.61 |
| 2200 | 38.80 | 38.87 | 208.8 | 209.96 | 68.61 | 69.52 |
| 2300 | 38.94 | 38.99 | 210.2 | 211.03 | 72.49 | 73.35 |
| 2400 | 39.07 | 39.14 | 211.6 | 212.58 | 76.39 | 77.29 |
| 2500 | 39.19 | 39.3 | 212.9 | 213.87 | 80.31 | 81.25 |
| 2600 | 39.31 | 39.45 | 214.1 | 215.06 | 84.23 | 85.19 |
| 2700 | 39.43 | 39.58 | 215.4 | 216.34 | 88.17 | 89.04 |
| 2800 | 39.55 | 39.72 | 216.5 | 217.48 | 92.12 | 93.11 |
| 2900 | 39.66 | 39.88 | 217.7 | 218.79 | 96.08 | 96.99 |
| 3000 | 39.77 | 40 | 218.8 | 219.75 | 100.0 | 101.03 |
| 3500 | 40.31 | 40.62 | 224.0 | 225.21 | 120.1 | 122.67 |
| 4000 | 40.85 | 41.17 | 228.7 | 230.16 | 140.4 | 142.37 |
| 4500 | 41.42 | 41.77 | 232.9 | 234.57 | 160.9 | 162.53 |
| 5000 | 42.04 | 42.41 | 236.7 | 238.64 | 181.8 | 183.02 |
| 5500 | 42.73 | 43.1 | 240.1 | 241.88 | 203.0 | 204.36 |
| 6000 | 43.51 | 43.82 | 243.4 | 244.96 | 224.5 | 226.1 |

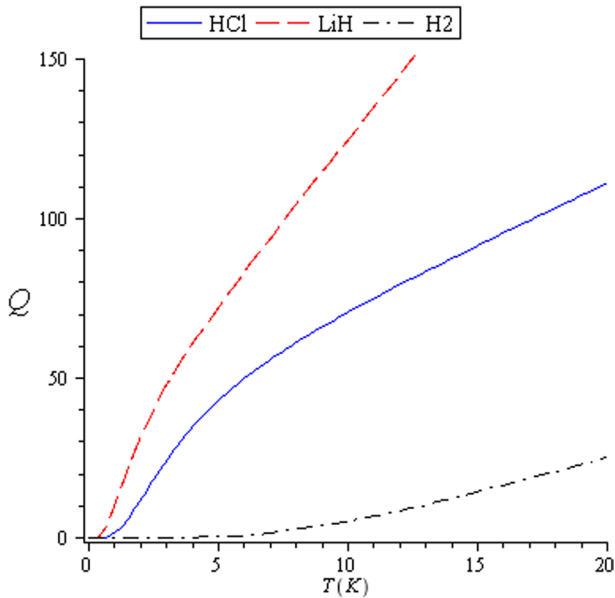
Figure 2 shows the partition function as a function of temperature for HCl, LiH and H₂. It is obvious from the figure that the partition function rises with increasing the temperature. The curves show a similar behavior, but LiH has higher values than the two others.

In Fig. 3, we have plotted the mean energy of diatomic molecules versus temperature. At low temperatures ($0 < T < 18K$), they have different behavior but at higher temperatures ($T > 18K$) have similar behavior and show a smooth treatment. We can see a bow at the curves. For LiH, it occurs at ($5.63K < T < 9.1K$), for HCl at ($6.86K < T < 10.11K$) and for H₂ at ($9.89K < T < 15.52K$). This behavior of diatomic molecules is due to their molecular structure. At $T < 15K$, we can see significant energy changes for three molecules but as temperature increases, they show less changes.

Figure 4 presents the specific heat at constant volume for diatomic molecules. It can be seen that the curves show a peak structure at low temperature, so at special temperature, the probability of a transition to higher levels is occur. With enhancing temperature, the system reaches more thermal energy, and hence, the probability increases. In this regard, a peak occurs in the specific heat when the energy difference between two levels and thermal energy are equal to each other. For each molecule, the peaks appear at different values of specific heat and it is related to the structure of molecules.

Table 5 Thermodynamic properties for H₂ using Hulthen-screened Kratzer potential compared with experimental data [45]

| Temperature (K) | C_p (J/mol*K) | | $-(G-H_{298.15})/T$ (J/mol*k) | | $H-H_{298.15}$ (kJ/mol) | |
|-----------------|-----------------|-------------|-------------------------------|-------------|-------------------------|-------------|
| | Exp | Our results | Exp | Our results | Exp | Our results |
| 300 | 28.85 | 29.27 | 130.7 | 131.12 | 0.05 | 0.06 |
| 400 | 29.18 | 29.63 | 131.8 | 132.04 | 2.96 | 3.09 |
| 500 | 29.26 | 29.76 | 134.0 | 134.3 | 5.88 | 6.12 |
| 600 | 29.32 | 29.82 | 136.4 | 136.8 | 8.81 | 8.99 |
| 700 | 29.44 | 29.5 | 138.8 | 139 | 11.75 | 11.93 |
| 800 | 29.62 | 29.72 | 141.2 | 141.38 | 14.70 | 14.97 |
| 900 | 29.88 | 29.93 | 143.4 | 143.55 | 17.68 | 17.83 |
| 1000 | 30.20 | 30.24 | 145.5 | 145.73 | 20.68 | 20.92 |
| 1500 | 32.30 | 32.45 | 154.7 | 154.96 | 36.29 | 36.05 |
| 2000 | 34.28 | 34.39 | 161.9 | 162.11 | 52.95 | 53.11 |
| 2500 | 35.84 | 35.98 | 168.0 | 168.47 | 70.50 | 70.74 |
| 3000 | 37.09 | 37.23 | 173.3 | 173.46 | 88.74 | 88.99 |
| 3500 | 38.15 | 38.51 | 178.0 | 178.59 | 107.6 | 107.85 |
| 4000 | 39.12 | 39.37 | 182.1 | 182.38 | 126.9 | 127.16 |
| 4500 | 40.02 | 40.19 | 185.9 | 185.17 | 146.7 | 146.98 |
| 5000 | 40.83 | 40.99 | 189.4 | 189.66 | 166.9 | 167.13 |
| 5500 | 41.50 | 41.68 | 192.6 | 192.88 | 187.5 | 187.82 |
| 6000 | 41.97 | 42.25 | 195.6 | 195.81 | 208.3 | 208.56 |

**Fig. 2** Partition function for diatomic molecules using Hulthen-screened Kratzer potential

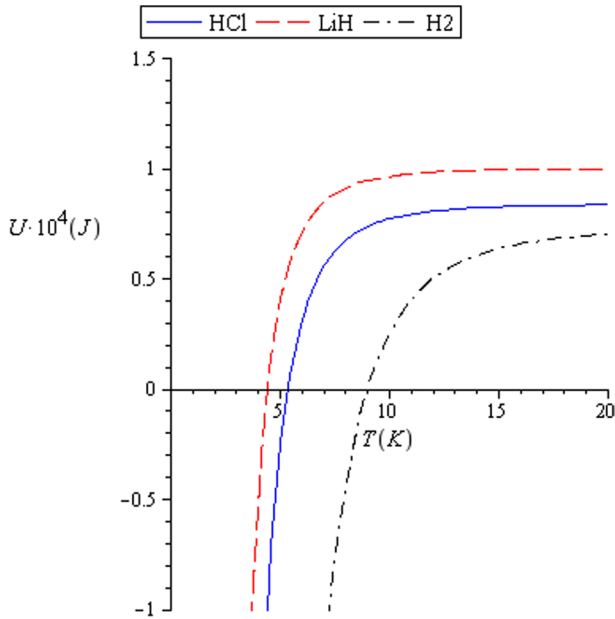


Fig. 3 Mean energy for diatomic molecules using Hulthen-screened Kratzer potential

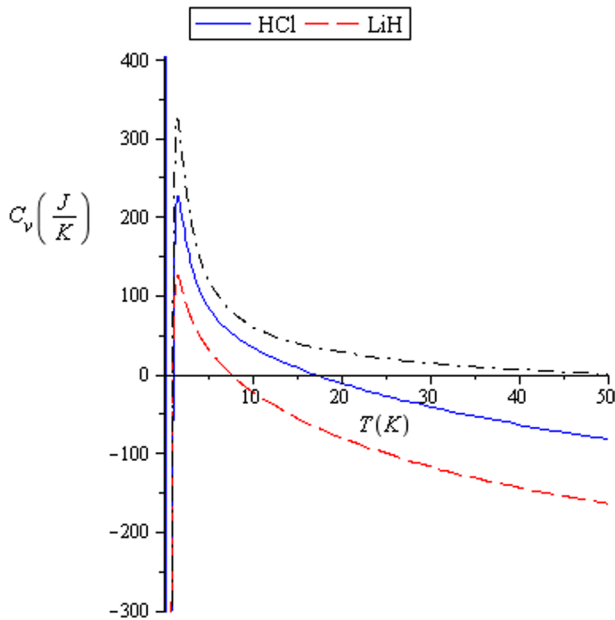


Fig. 4 Specific heat at constant volume for diatomic molecules using Hulthen-screened Kratzer potential

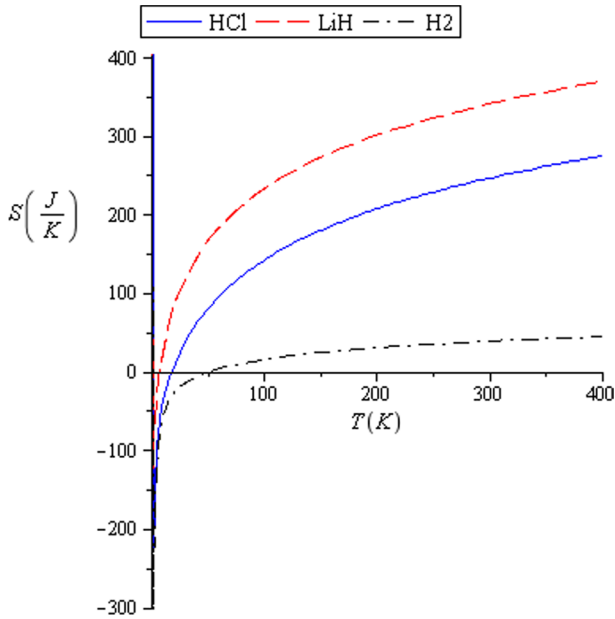


Fig. 5 Entropy for diatomic molecules using Hulthen-screened Kratzer potential

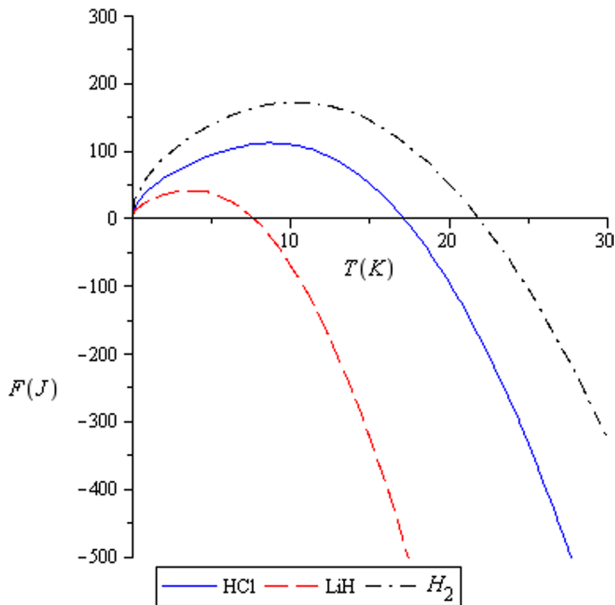


Fig. 6 Free energy for diatomic molecules using Hulthen-screened Kratzer potential

In Fig. 5, we have plotted the entropy of diatomic molecules as a function of temperature. It is observed that the entropy for 3 cases is enhanced with increasing the temperature. It reflects the subject that the interaction potential increases the disorder of the system.

Figure 6 displays free energy of the diatomic molecules versus temperature. One can see that the curves show similar treatment. With increasing the temperature, first, they increase, and then, they decrease.

4 Conclusions

In this work, we have solved the SE with the Hulthén plus screened Kratzer potential model using a suitable approximation and have obtained the energy spectra of the model. Using the energy spectra of the potential, the partition function and other thermodynamic properties have been calculated using the Poisson summation formula. With these results, the specific heat at constant pressure, enthalpy and Gibbs free energy of diatomic molecules like HCl, LiH and H₂ have been studied graphically and compared with reported experimental data. There is a good agreement between them. Also, we have studied other thermodynamic properties such as mean energy, specific heat at constant volume, entropy and free energy for the diatomic molecules and show the behavior of the potential model.

Appendix: Nikiforov–Uvarov method

We use the Nikiforov–Uvarov method to solve the second-order differential equation with an appropriate transformation $S = S(r)$ [44]. It is given as follows

$$\frac{d^2\Psi_n(s)}{ds^2} + \frac{\tilde{\tau}(s)}{\sigma(s)} \frac{d\Psi_n(s)}{ds} + \frac{\tilde{\sigma}(s)}{\sigma^2(s)} \Psi_n(s) = 0 \quad (22)$$

where $\sigma(s)$ and $\tilde{\sigma}(s)$ are second-degree polynomials and $\tilde{\tau}(s)$ is a first-degree polynomial. By using the transformation $\Psi_n(s) = \Phi(s)y_n(s)$ and considering separation of variables, Eq. (1) reduces to an equation of the hypergeometric function as

$$\sigma(s) \frac{d^2y_n(s)}{ds^2} + \tau(s) \frac{dy_n(s)}{ds} + \lambda y_n(s) = 0 \quad (23)$$

Here, $y_n(s)$ is the hypergeometric-type function. The polynomial solution of Eq. (23) is given by the Rodrigues relation

$$y_n(s) = \frac{B_n}{\rho(s)} \frac{d^n}{ds^n} [\sigma^n(s)\rho(s)] \quad (24)$$

where B_n is the normalization constant. The weight function, $\rho(s)$, must satisfy the following condition [44]

$$\frac{dw(s)}{ds} = \frac{\tau(s)}{\sigma(s)} w(s); w(s) = \sigma(s)\rho(s) \quad (25)$$

Also, $\Phi(s)$ is defined by its logarithmic derivative relation as

$$\frac{\Phi'(s)}{\Phi(s)} = \frac{\pi(s)}{\sigma(s)} \quad (26)$$

In this method, we need to define the function $\pi(s)$ and the parameter λ . So, we have

$$\pi(s) = \frac{\sigma' - \tilde{\tau}}{2} \pm \sqrt{\left(\frac{\sigma' - \tilde{\tau}}{2}\right)^2 - \tilde{\sigma} + k\sigma} \quad (27)$$

$$\lambda = k + \pi'(s) \quad (28)$$

To determine the value of k , the expression under the square root must be a square of a polynomial. Therefore, a new eigenvalue equation is given by

$$\lambda = \lambda_n = -n\tau' - \frac{n(n-1)}{2}\sigma^n \quad (29)$$

where

$$\tau(s) = \tilde{\tau}(s) + 2\pi(s) \quad (30)$$

Author Contributions AG took care of methodology, formal analysis, project administration, software and writing original draft. SMJ review of the manuscript.

Declarations

Competing interests The authors declare no competing interests.

Conflict of interest Not applicable.

Ethical Approval Not applicable.

References

1. R. Khordad, A. Ghanbari, Analytical calculations of thermodynamic functions of lithium dimer using modified Tietz and Badawi-Bessis-Bessis potentials. *Comput. Theor. Chem.* **1155**, 1–8 (2019)
2. R. Khordad, A. Avazpour, A. Ghanbari, Exact analytical calculations of thermodynamic functions of gaseous substances. *Chem. Phys.* **517**, 30–35 (2019)
3. K.-X. Fu, M. Wang, C.-S. Jia, Improved five-parameter exponential-type potential energy model for diatomic molecules. *Commun. Theor. Phys.* **71**, 103 (2019)
4. A. Akour, Thermodynamic properties of low-density Xe gas in the temperature range 165–275 K. *Int. J. Thermophys.* **39**, 9 (2018)

5. Y. Zhou, E.W. Lemmon, Equation of state for the thermodynamic properties of 1, 1, 2, 2, 3-pentafluoropropane (R-245ca). *Int. J. Thermophys.* **37**, 27 (2016)
6. R. Khordad, A. Ghanbari, Theoretical prediction of thermodynamic functions of TiC: morse ring-shaped potential. *J. Low Temp. Phys.* **199**, 1–13 (2020)
7. V.L. Zherebtsov, M.M. Peganova, Water solubility versus temperature in jet aviation fuel. *Fuel* **102**, 831–834 (2012)
8. N.P. Stadie, M. Murialdo, C.C. Ahn, B. Fultz, Anomalous isosteric enthalpy of adsorption of methane on zeolite-templated carbon. *J. Am. Chem. Soc.* **135**, 990–993 (2013)
9. S.A. Moses, J.P. Covey, M.T. Miecznikowski, B. Yan, B. Gadway, J. Ye, D.S. Jin, Creation of a low-entropy quantum gas of polar molecules in an optical lattice. *Science* **350**, 659–662 (2015)
10. R. Mebsout, S. Amari, S. Mécabih, B. Abbar, B. Bouhafs, Spin-polarized calculations of magnetic and thermodynamic properties of the full-Heusler Co_2MnZ (Z= Al, Ga). *Int. J. Thermophys.* **34**, 507–520 (2013)
11. J. Wang, C.-S. Jia, C.-J. Li, X.-L. Peng, L.-H. Zhang, J.-Y. Liu, Thermodynamic properties for carbon dioxide. *ACS Omega* **4**, 19193–19198 (2019)
12. A. Ghanbari, R. Khordad, F. Taghizadeh, Influence of Coulomb term on thermal properties of fluorine. *Chem. Phys. Lett.* **801**, 139725 (2022)
13. U. Okorie, A. Ikot, E. Chukwuocha, M. Onyeaju, P. Amadi, M. Sithole, G. Rampho, Energies Spectra and thermodynamic properties of Hyperbolic Pöschl-Teller potential (HPTP) model. *Int. J. Thermophys.* **41**, 1–15 (2020)
14. U.S. Okorie, A.N. Ikot, E.O. Chukwuocha, G. Rampho, Thermodynamic properties of improved deformed exponential-type potential (IDEP) for some diatomic molecules. *Results Phys.* **17**, 103078 (2020)
15. K.R. Purohit, R.H. Parmar, A.K. Rai, Bound state solution and thermodynamic properties of the screened cosine Kratzer potential under influence of the magnetic field and Aharanov-Bohm flux field. *Ann. Phys.* **424**, 168335 (2021)
16. L.H. Zhang, X.P. Li, C.S. Jia, Approximate solutions of the Schrödinger equation with the generalized Morse potential model including the centrifugal term. *Int. J. Quantum Chem.* **111**, 1870–1878 (2011)
17. M. Hamzavi, S.M. Ikhdaïr, K.-E. Thylwe, Equivalence of the empirical shifted Deng-Fan oscillator potential for diatomic molecules. *J. Math. Chem.* **51**, 227–238 (2013)
18. O. Mustafa, A new deformed Schiöberg-type potential and ro-vibrational energies for some diatomic molecules. *Phys. Scr.* **90**, 065002 (2015)
19. H. Boukabcha, M. Hachama, A. Diaf, Ro-vibrational energies of the shifted Deng-Fan oscillator potential with Feynman path integral formalism. *Appl. Math. Comput.* **321**, 121–129 (2018)
20. A. Amrouche, A. Diaf, M. Hachama, Path integral treatment of the deformed Schiöberg-type potential for some diatomic molecules. *Can. J. Phys.* **95**, 25–30 (2017)
21. E. Inyang, E. William, J. Obu, Eigensolutions of the N-dimensional Schrödinger equation interacting with Varshni-Hulthen potential model. *Revista mexicana de física* **67**, 193–205 (2021)
22. A.N. Ikot, C.O. Edet, U.S. Okorie, A.-H. Abdel-Aty, M. Ramantswana, G.J. Rampho, N.A. Alshehri, S. Elagan, S. Kaya, Solutions of the 2D Schrodinger equation and its thermal properties for improved ultra-generalized exponential hyperbolic potential (IUGE-HP). *Eur. Phys. J. Plus* **136**, 1–18 (2021)
23. A. Ghanbari, R. Khordad, Bound states and optical properties for Derjaguin-Landau-Verweij-Overbook potential. *Opt. Quant. Electron.* **53**, 1–11 (2021)
24. A. Ghanbari, R. Khordad, Theoretical prediction of thermodynamic properties of N2 and CO using pseudo harmonic and Mie-type potentials. *Chem. Phys.* **534**, 110732 (2020)
25. K.R. Purohit, R.H. Parmar, A.K. Rai, Eigensolution and various properties of the screened cosine Kratzer potential in D dimensions via relativistic and non-relativistic treatment. *Eur. Phys. J. Plus* **135**, 1–38 (2020)
26. K.R. Purohit, R.H. Parmar, A.K. Rai, Energy and momentum eigenspectrum of the Hulthen-screened cosine Kratzer potential using proper quantization rule and SUSYQM method. *J. Mol. Model.* **27**, 1–23 (2021)
27. K.R. Purohit, R.H. Parmar, A.K. Rai, Solution of the modified Yukawa-Kratzer potential under influence of the external fields and its thermodynamic properties. *J. Math. Chem.* **60**, 1930–1982 (2022)
28. P.M. Morse, Diatomic molecules according to the wave mechanics. II. Vibrational levels. *Phys. Rev.* **34**, 57 (1929)

29. E.D. Davis, Uniform approximation of wave functions with improved semiclassical transformation amplitudes and Gram-Schmidt orthogonalization. *Phys. Rev. A* **70**, 032101 (2004)
30. H. Konwent, P. Machnikowski, P. Magnuszewski, A. Radosz, Some properties of double-Morse potentials. *J. Phys. A Math. Gen.* **31**, 7541 (1998)
31. C. Edet, U. Okorie, G. Osobonye, A. Ikot, G. Rampho, R. Sever, Thermal properties of Deng–Fan–Eckart potential model using poisson summation approach. *J. Math. Chem.* **58**, 989–1013 (2020)
32. X.-Y. Chen, J. Li, C.-S. Jia, Thermodynamic properties of gaseous carbon disulfide. *ACS Omega* **4**, 16121–16124 (2019)
33. C. Onate, J. Ojonubah, Relativistic and nonrelativistic solutions of the generalized Pöschl-Teller and hyperbolical potentials with some thermodynamic properties. *Int. J. Modern Phys. E* **24**, 1550020 (2015)
34. R. Khordad, B. Mirhosseini, M. Mirhosseini, Thermodynamic properties of a GaAs quantum dot with an effective-parabolic potential: theory and simulation. *J. Low Temp. Phys.* **197**, 95–110 (2019)
35. F. Nammass, A. Sandouqa, H. Ghassib, M. Al-Sugheir, Thermodynamic properties of two-dimensional few-electrons quantum dot using the static fluctuation approximation (SFA). *Physica B* **406**, 4671–4677 (2011)
36. R. Khordad, Thermodynamical properties of triangular quantum wires: entropy, specific heat, and internal energy. *Continuum Mech. Thermodyn.* **28**, 947–956 (2016)
37. D. Nath, A.K. Roy, Ro-vibrational energy and thermodynamic properties of molecules subjected to Deng-Fan potential through an improved approximation. *Int. J. Quantum Chem.* **121**, e26616 (2021)
38. U. Okorie, A. Ikot, G. Rampho, P. Amadi, H.Y. Abdullah, Analytical solutions of fractional Schrödinger equation and thermal properties of Morse potential for some diatomic molecules. *Mod. Phys. Lett. A* **36**, 2150041 (2021)
39. Q.-C. Ding, C.-S. Jia, J.-Z. Liu, J. Li, R.-F. Du, J.-Y. Liu, X.-L. Peng, C.-W. Wang, H.-X. Tang, Prediction of thermodynamic properties for sulfur dimer. *Chem. Phys. Lett.* **803**, 139844 (2022)
40. I.B. Okon, O.O. Popoola, E. Omugbe, A.D. Antia, C.N. Isonguyo, E.E. Ituen, Thermodynamic properties and bound state solutions of Schrodinger equation with Mobius square plus screened-Kratzer potential using Nikiforov-Uvarov method. *Comput. Theor. Chem.* **1196**, 113132 (2021)
41. E.P. Inyang, E.P. Inyang, I. Akpan, J. Ntibi, E. William, Masses and thermodynamic properties of a Quarkonium system. *Can. J. Phys.* **99**, 982–990 (2021)
42. E. Inyang, P. Iwuji, J.E. Ntibi, E. William, E. Ibang, Solutions of the Schrödinger equation with Hulthén-screened Kratzer potential: application to diatomic molecules. *East Eur. J. Phys.* **2**, 12–22 (2022)
43. R. Greene, C. Aldrich, Variational wave functions for a screened Coulomb potential. *Phys. Rev. A* **14**, 2363 (1976)
44. A.F. Nikiforov, V.B. Uvarov, *Special functions of mathematical physics* (Springer, 1988)
45. P. Linstorm, NIST chemistry webbook, NIST standard reference database number 69. *J. Phys. Chem. Ref. Data Monogr.* **9**, 1–1951 (1998)
46. O. Oluwadare, K. Oyewumi, Energy spectra and the expectation values of diatomic molecules confined by the shifted Deng-Fan potential. *Eur. Phys. J. Plus* **133**, 422 (2018)

Publisher's Note Springer Nature remains neutral with regard to jurisdictional claims in published maps and institutional affiliations.

Springer Nature or its licensor (e.g. a society or other partner) holds exclusive rights to this article under a publishing agreement with the author(s) or other rightsholder(s); author self-archiving of the accepted manuscript version of this article is solely governed by the terms of such publishing agreement and applicable law.